CAFEE
CENTER FOR ALTERNATIVE FUELS, ENGINES AND EMISSIONS
West Virginia University

Final Report

Fuel consumption and emissions testing of a best-in-class tractor-trailer in the US

Submitted to:
International Council on Clean Transportation (ICCT)

Prepared by:
Arvind Thiruvengadam (Joint-Principal Investigator)
Marc C. Besch (Joint-Principal Investigator)
Berk Demirgök (Co-Principal Investigator)
Dan Carder (Co-Principal Investigator)
Cem Baki

Center for Alternative Fuels, Engines & Emissions
Dept. of Mechanical & Aerospace Engineering
West Virginia University
Morgantown WV 26506-6106

May 15, 2018

ACKNOWLEDGMENT

WVU would like to thank Felipe Rodriguez and Oscar Delgado from the International Council on Clean Transportation for their valuable and vital input during the course of this project as well as providing their expertise and support in regards to the coastdown procedure and understanding the workings of the VECTO simulation tool.

WVU thanks ICCT for providing the funding for this research project.

TABLE OF CONTENTS

Acknowledgment 1
Table of Contents 1
List of Tables 1
LIST OF FIGURES 1
1 Introduction 1
2 Methodology 1
2.1 Selection of vehicle 1
2.2 Air drag measurements 2
2.2.1 Constant Speed Test 3
2.2.2 Coastdown Test 6
2.3 Chassis dynamometer testing 12
2.3.1 Test Fuel Specifications 12
2.3.2 Test Cycles 12
2.3.3 Chassis Dynamometer Measurements 15
2.3.4 Test Procedures 16
2.4 Data evaluation 18
3 Results and Discussion 1
3.1 Average Wheel Work 1
3.2 Fuel Consumption 2
3.3 Steady-state Engine Mapping Results 3
4 References 1

LIST OF TABLES

Table 2.1: Specifications of the tractor. 2
Table 2.2: Test trailer specifications 2
Table 2.3: Weather conditions during CST. 3
Table 2.4: Measurement systems and instruments. 4
Table 2.5: Specifications of high resolution wheel torque meter TWHR2000 4
Table 2.6: Results for the constant speed testing methodology 6
Table 2.7: Vehicle speed ranges applied during coastdown testing. 7
Table 2.8: Weather conditions during coastdown testing. 7
Table 2.9: Results of tire rolling resistance test. 8
Table 2.10: Results of the coastdown tests. 8
Table 2.11: Upper and lower limits for validation. 9
Table 2.12: Comparison drag area results between constant speed and coastdown methods. 10
Table 2.13: ULSD test fuel specifications. 12
Table 2.14: Chassis dynamometer test cycle characteristics. 13
Table 2.15: Specifications of heavy-duty chassis dynamometer at ARB facility, Sacramento, CA. 15
Table 2.16: Measurement systems and parameters [5] 16
Table 2.17: Chassis dynamometer warm-up procedure. 17
Table 3.2: Selected steady-state test points 3

LIST OF FIGURES

Figure 2.1: High resolution wheel torque meters installed on test vehicle. 5

Figure 2.2: Yaw angle correction function over an interval of yaw angle = 0 to 1º; '*orange square*' indicating actual coastdown results from this study. 10

Figure 2.3: Drag area vs. yaw angle for different measurement methods. 11

Figure 2.4: Chassis dynamometer test cycles: a) VECTO long haul, b) VECTO regional delivery, c) GEM 55 with grade, and d) GEM ARB transient cycle. 14

Figure 2.5: Losses estimated from chassis dynamometer calibration procedure. 18

Figure 3.1: Comparison of distance-specific positive wheel work in [kWh/km] between experimental results and simulations for the different chassis dynamometer cycles. 1

Figure 3.2: Comparison of distance-specific fuel consumption between gravimetric and ECU-broadcasted calculation methods in [L/100km] for the different chassis dynamometer cycles. 2

Figure 3.3: Comparison of work-specific fuel consumption between gravimetric and ECU-broadcasted calculation methods in [g/kWh] for the different chassis dynamometer cycles. 2

Figure 3.4 Comparison of CO_2 emissions in [g/t-km] between the different chassis dynamometer cycles. 3

Figure 3.5: Steady-state brake-specific fuel consumption in [g/kWh] calculated through gravimetric fuel measurement and ECU derived engine work. 4

Figure 3.6: Steady-state brake-specific fuel consumption in [g/kWh] calculated through ECU-broadcasted fuel measurement and ECU derived engine work. 5

Figure 3.7: Steady-state engine thermal brake efficiency [%] calculated through gravimetric fuel measurement and ECU derived engine work. 6

1 INTRODUCTION

The primary objective of this study was to conduct aerodynamic testing on a closed test track along with chassis dynamometer testing of a US heavy-duty Diesel (HDD), Class 8 tractor to assess the fuel consumption over prescribed driving cycles. The air drag was measured following the coastdown (CD) procedure specified in US regulation [1], as well as the constant speed tests (CST) defined in the European regulation [2]. The results were used to determine speed-based road load forces onto the vehicle for subsequent chassis dynamometer testing.

2 METHODOLOGY

This chapter will discuss the selection of the test vehicle and its specifications in the first Section 2.1, followed by a discussion of the constant speed test and coastdown methodology for air drag evaluation in Sections 2.2.1 and 2.2.2, respectively. Finally, Section 2.3 will present the vehicle chassis dynamometer testing procedure employed during the herein presented study.

2.1 Selection of vehicle

The tractor and trailer combination was selected to represent the 'best-available' technology in 2015, as evaluated with the support of the manufacturer, and which exhibits significant market presence in the United States (US). The Center for Alternative Fuels, Engines and Emissions (CAFEE) was able to recruit a suitable heavy-duty Diesel Class 8 tractor directly from the respective OEM. In conjunction with the tractor, a conventional US trailer was selected that was outfitted with side-skirts for aerodynamic enhancement. Table 2.1 provides the specifications of the tractor selected for this study. The engine specifications are provided in ranges in order to conceal the model and make of the truck being tested.

The trailer used during the air drag measurement was equipped with 2 axles, with spring rides, and a composite plate van. All specifications of the test trailer were compliant with the provisions stipulated in the US regulation for testing of heavy-duty motor vehicles [3] as listed in Table 2.2.

Table 2.1: Specifications of the tractor.

Vehicle Class	Class 8
Cabin Type	Sleeper Cab, High Roof
Engine Volume [liter]	14 to 15
Number of Cylinders	Inline 6
Engine Torque [Nm]	2170 to 2440
Engine Power [kW]	298 to 315
Engine Idle Speed [rpm]	600
Engine Technology Features	Amplified Common Rail System, Asymmetric Turbocharger, Variable Speed Water Pump
Emission Standard	US-EPA 2010
Emission Control	EGR, DOC, DPF, SCR
Transmission Type	AMT
Number of Gears	12
Axle Configuration	6x4
Axle Type	Tandem Rear Axle
1st and 12th Gear Ratios	14.928 and 1.000
Axle Ratio	2.41
GVW [metric ton]	20.4
Vehicle curb mass [metric ton]	9.26

Table 2.2: Test trailer specifications.

Length [m]	16.1
Width [m]	2.6
Height [m]	4.1
Empty weight [metric ton]	7.95
Side skirts	Fuel efficient, aerodynamic advanced trailer skirt - U.S. EPA Verified SmartWay Technology
Tires	295/75R 22.5 low rolling resistance radial tires - U.S. EPA Verified SmartWay Technology

2.2 Air drag measurements

There are two different approaches to determine the drag coefficient, specifically, the constant speed test (CST) as well as the coastdown (CD) test methods. These procedures are defined in the Annex VIII of the European HDV CO_2 legislation [2] and US Phase 2 GHG regulation [3]. In the following, Sections 2.2.1 and 2.2.2 will provide detailed test procedures and results for the two air drag measurement methodologies, respectively.

Air drag measurements were completed at Michelin's Laurens Proving Ground facility in Laurens, SC, USA. Track 9 was the most suitable track for constant speed and coastdown tests at this facility and is characterized by a 1463 meters straight section, with near perfect flatness, and a track width of 12 to 20 meters. The straight center section of the track was connected to two loops at each end allowing for the vehicle to return and accelerate back to the measurement section without coming to a halt. The surface texture of Track 9 was smooth at a macro scale and rough at a micro scale.

2.2.1 Constant Speed Test

Following the provisions stipulated in the EU for the aerodynamic testing of heavy-duty vehicles [2], WVU performed a constant speed test to determine the total forces onto the vehicle at two different speeds. The direct measurement of the road-load forces is necessary for the calculation of aerodynamic drag and tire rolling resistance in the CST method. For this purpose, an appropriate wheel torque meter was used to measure the wheel forces. Since the test vehicle has two driven axles (i.e. 6x4 axle configuration), both axles were equipped with wheel torque meters. The wheel torque meter was attached to the drive axles and the vehicle was operated at two different constant speeds. The weather condition during CST was suitable to perform testing. All weather conditions were compliant with the EU regulatory requirements [2] as shown in Table 2.3. Weather data was collected from the Michelin Laurens Proving Ground's stationary weather measurement station. Additionally, a Gill Instrument Windsonic 75 anemometer was positioned on the test track to determine the wind speed and direction at the measurement section following requirement outlined in 40 CFR §1037 [1]. Track surface temperature during the tests were measured at around 25 ℃.

Table 2.3: Weather conditions during CST.

Track surface condition	Dry
Average ambient temperature	19.7 ℃
Average wind speed	1.5 m/s
Average barometric pressure	1031.0 mbar
Average relative humidity	38.1%
Average track surface temperature	25 ℃

A second Gill Instrument Windsonic 75 anemometer was placed at a height of 1.5 meters above the top surface of the trailer to measure air speeds as the vehicle was driving down the test section. A K-Type thermocouple was placed on the pole of anemometer in order to determine the ambient air temperature. Proving ground surface temperatures were periodically measured manually with an infrared temperature sensor during the tests to ensure that the surface temperature was compliant with the regulatory requirements. Table 2.4 lists the equipment used for CST.

Table 2.4: Measurement systems and instruments.

Wheel Torque Transducer	Michigan Scientific Corporation TWHR2000
Vehicle Speed	CAN bus and GPS
Engine Speed	CAN bus
Vehicle Position	GPS
Mobile Anemometer	Gill Instrument Windsonic 75
Ambient Temperature Sensor	K-type thermocouple

For measuring torque at the wheel hubs a high resolution wheel torque measurement system form Michigan Scientific Corporation (model TWHR2000) was used. The specifications related to the torque measurement equipment are summarized in Table 2.5. Figure 2.1 depicts the wheel torque transducers installed on the drive axles of the test vehicle. During the course of testing, no optoelectronic barriers were used for triggering the start and end points of the measurement sections as they were not available. However, instead of optoelectronic barriers, GPS location was used to determine the start and end points of the measurement section.

Table 2.5: Specifications of high resolution wheel torque meter TWHR2000.

Manufacturer	Michigan Scientific Corporation
Model	TWHR2000
Maximum Load Capacity	±27,000 Nm
Full Scale Measurable Load	±2,700 Nm
Accuracy	3 Nm
Sensor	4 arm strain-gage bridge
Nonlinearity	0.12% of full scale output
Hysteresis	0.05% of full scale output
Temperature Range, Compensated	-40 °C to 93 °C
Temperature Range, Practical	-40 °C to 149 °C
Excitation Voltage, Maximum	10VDC

Figure 2.1: High resolution wheel torque meters installed on test vehicle.

The raw data collected during the CST was post-processed using the European Union's (EU) VECTO Air Drag Tool. The post-processing tool performs the data validation, filtering, and calibration, as well as the calculation of the air drag coefficient, corrected to zero yaw angle. The air drag results from the CST are shown in Table 2.6.

Table 2.6: Results for the constant speed testing methodology

Test Track Condition	$[-]$	Dry
Average Ambient Temperature	℃	19.7
Average Vehicle Speed (LS)	$[km/h]$	14.1
Average Vehicle Speed (HS)	$[km/h]$	89.1
CdxA without correction	$[m^2]$	5.238
Average yaw angle	[°]	0.83
CdxA cross wind correction	$[m^2]$	-0.057
CdxA correction for anemometer influence	$[m^2]$	-0.15
CdxA measured [1]	$[m^2]$	5.031
Vehicle height	$[m]$	4.06
Frontal area [2]	$[m^2]$	10.45
Cd value [3]	$[-]$	0.481

2.2.2 Coastdown Test

For the coastdown methodology, the test procedure described in the US GHG Phase 2 regulation [1] was followed to calculate drag area (i.e. *CdxA*). Coastdown tests were executed just after CSTs at the same proving ground and track (i.e. Track 9). The coastdown procedure was split into a separate high-speed and two low-speed portions (i.e. one low-speed test each direction) as the total length of the truck was not sufficient to perform a full coastdown between 112 to 16km/h. In total, 6 high-speed and accompanying low-speed passes per direction (i.e. North-South and South-North) were completed. Table 2.7 illustrates the speed ranges applied during coastdown testing. At the start of coastdown testing, the track surface was slightly wetted due to changes in weather conditions with the onset of light rain. However, after the combination of sixth of high- and low-speed test runs, the weather conditions have worsened to the extent that continuous rainfall did not allow to continue testing, as hydroplane and water splash were observed. Thus, no

[1] *CdxA* measured value is after yaw angle and anemometer influence correction, however, does not include the anemometer height correction to account for boundary layer influences (5.238-0.057-0.15=5.031).

[2] Since the trailer was higher than the tractor, the trailers frontal area used for calculations. Height and width of the trailer were manually measured.

[3] Drag coefficient (Cd) was obtained by dividing the drag area by the frontal area. (5.031/10.45=0.481).

more than 6 passes for both high- and low-speed ranges were completed. The weather conditions during coastdown testing are summarized in Table 2.8.

Table 2.7: Vehicle speed ranges applied during coastdown testing.

Coastdown Section		Upper speed limit [km/h]	Lower speed limit [km/h]	Nominal speed [km/h]
High speed range	Start point	115.9	109.4	112.6
	End point	99.8	93.3	96.5
Low speed range	Start point	35.4	29.0	32.2
	End point	19.3	12.9	16.1

Table 2.8: Weather conditions during coastdown testing.

Track surface condition	Wet
Average ambient temperature	14.3 °C
Average wind speed	0.44 m/s
Average barometric pressure	1027.0 mbar
Average relative humidity	50.5%
Average track surface temperature	25 °C

For the post-processing and analysis of the coastdown data, it was necessary to estimate the speed dependence of the frictional losses of the drive axles and the tires. The following points provide further details on the approach followed:

- There was no data available for axle power losses for the test vehicle. Therefore, to calculate the speed dependency of the spin losses, the default axle loss map included in the US regulatory simulation tool, GEM, was utilized.
- In order to determine the tire rolling resistance coefficients of the drive axle tires, they were sent to Smithers Rapra North America's Ravenna Laboratory (Ravenna, OH) to measure the rolling resistance over the '*Stepwise Coastdown Methodology for Measuring Tire Rolling Resistance*' defined in the SAE J2452 standard. The results of the test provide the regression coefficients required to estimate the rolling resistance at different speeds. Equation 1 provides the calculation of the tire rolling resistance,

where, n_t is the number of tires, P the set inflation pressure, L the load over the axle, and finally, v the average segment speed.

$$F_{TRR} = n_t . P^{\alpha} . \left(\frac{L}{n_t}\right)^{\beta} . (a + b . \bar{v} + c . \bar{v}^2) \quad \text{Eq. (1)}$$

The coefficients obtained from this test are given at Table 2.9 and were used in the post-processing and analysis of the coastdown data.

Table 2.9: Results of tire rolling resistance test.

α	β	a	b	c
-0.4398	1.0420	0.0498	0.00010871	0.00000085

- Rotational wheel speed was measured with speed encoders as part of the wheel torque transducers (i.e. Michigan Scientific Corporation TWHR2000).
- Wind speed and direction was measured with Gill Instrument Windsonic 75 anemometer which was positioned just near the measurement section.
- Test data were collected at a frequency of 10 Hz.

Results of the coastdown tests are tabulated in Table 2.10.

Table 2.10: Results of the coastdown tests.

	Test Number	1	2	3	4	5	6
North to South Direction	Drag Area (Cd*A) (m^2)	4.686	4.605	4.679	4.507	4.609	-
	Drag Coefficient (Cd)	0.448	0.441	0.448	0.431	0.441	-
	Average Yaw Angle (°)	0.440	0.896	0.191	0.727	0.095	-
South to North Direction	Drag Area (Cd*A) (m^2)	4.636	4.605	4.431	4.478	4.753	4.656
	Drag Coefficient (Cd)	0.444	0.441	0.424	0.429	0.455	0.446
	Average Yaw Angle (°)	0.645	0.303	0.955	0.266	0.817	1.234

The calculated median of yaw angles was found to be 0.64°. Following the provisions set forth by CFR §1037.528 [1], the validation criteria for yaw angle was set to ±1° of the median yaw angle. The drag area validation criteria is ±2.0 standard deviations (σ). Tabulated upper and lower limits for yaw angle and drag area can be found in Table 2.11.

Table 2.11: Upper and lower limits for validation.

Parameter	Lower Limit	Average	Upper Limit
Yaw Angle	-0.36°	0.6°	1.64°
Drag Area	$4.420m^2$	$4.604m^2$ (σ =0.0922)	$4.7885m^2$

As it can be observed from Table 2.11, all tests are within the validation range and no outlier elimination was needed. After checking for test validity, effective drag area was calculated as 4.604 m^2 and effective yaw angle was calculated as 0.6°, respectively. According to requirements specified in 40 CFR, Part 1037 [1], there should be at least 24 points remaining after elimination of outliers. However, as mentioned earlier due to the deteriorating weather conditions (i.e. onset of increased rainfall) while performing the coastdown tests, it was not possible to safely conduct more than 11 passes per direction and vehicle speed range.

In order to be able to compare drag area results obtained through the US GHG Phase 2 regulatory procedures [1] with results from their European counterpart [2] the drag area from the coastdown tests was corrected to '*zero*' yaw angle using the regression coefficients applicable for tractor-trailers in the EU constant speed test procedure. The yaw angle correction function[4] is visualized in Figure 2.2. For a measured yaw angle of 0.6º obtained from the coastdown testing a drag area correction factor of 0.032m^2 was found. After exclusion of the yaw angle effect, the final drag area was determined to be 4.572m^2 with an associated drag coefficient (C_d) for zero yaw angle of 0.438.

A direct comparison between the drag area results obtained through the US GHG Phase 2 promulgated procedure [1] (i.e. coastdown method) and through EU regulatory requirements [2] (i.e. constant speed test method) is provided in Table 2.12.

[4] $Drag\ Area\ Difference = 0.030042\Psi + 0.040817\Psi^2 - 0.00213\Psi^3$

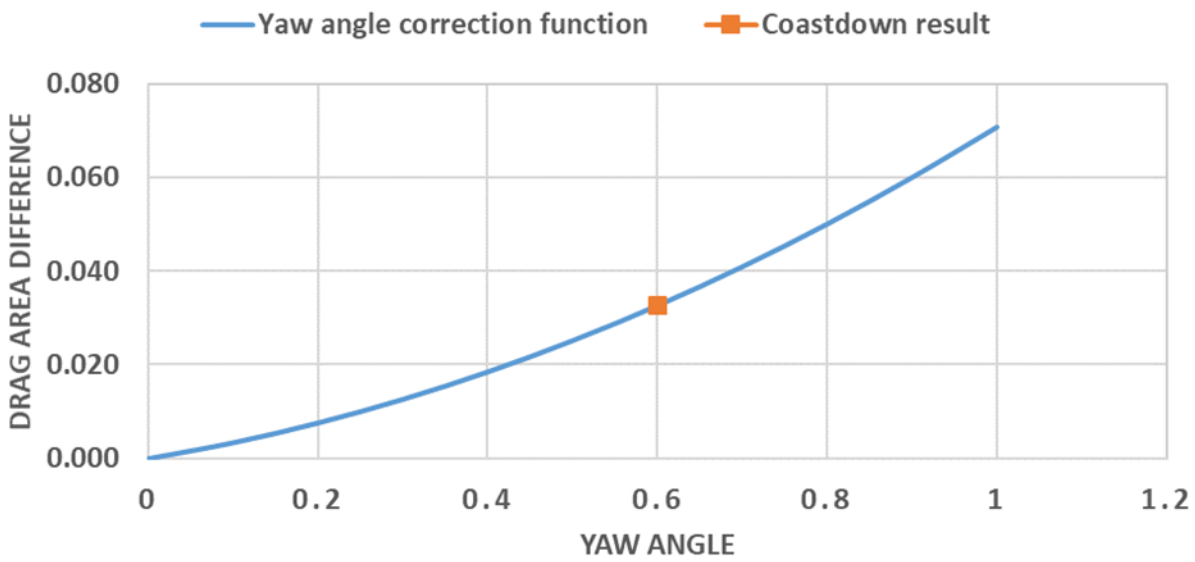

Figure 2.2: Yaw angle correction function over an interval of yaw angle = 0 to 1º; '*orange square*' indicating actual coastdown results from this study.

As can be seen from the Table 2.12, the air drag measurements following the US GHG Phase 2 regulatory procedure [1] yields a 9.1% lower drag coefficient value as compared to the air drag value measured following the EU regulatory requirements [2].

Table 2.12: Comparison drag area results between constant speed and coastdown methods.

		Yaw Angle [º]		
		0.83	0.6	Corrected Value for 0º
Drag Area (*CdxA*)	US GHG Phase 2 regulation [1], CD	-	4.604 m^2	4.572 m^2
	EU regulatory requirements [2], CST	5.088 m^2	-	5.031 m^2
	Percent Difference (w.r.t CST)			***9.1 %***

Figure 2.3 shows the comparison calculated drag areas between i) individual coastdown runs, ii) coastdown results without yaw angle correction, iii) coastdown results with yaw angle correction, iv) uncorrected CST, and finally v) corrected CST. A similar comparison exercise between the US Phase 2 coastdown procedure and the European constant speed test was recently performed by Rexeis et al. [4]. Their report concludes that drag area is highly dependent on yaw angle. However, in the herein presented study it was not possible to observe this dependency due

to very little variation of yaw angle between tests, resulting from the very calm wind conditions. Therefore, the difference between uncorrected and corrected (i.e. accounting for yaw angle effects) drag areas is not significant. As can be seen from the Table 2.12 the US GHG Phase 2 regulatory [1] procedure yields a 9.1% lower drag coefficient value as opposed to following the EU regulatory procedure [2]. Rexeis et al. [4] found a 13% lower drag area from the US Phase 2 coastdown method in comparison to the EU constant speed test. They argued that the assumption of constant rolling resistance (i.e., not dependent on the tire rotational speed) used in the EU constant speed test method results in higher air drag estimates. In this regard, the results obtained by this study are consistent with findings by Rexeis et al. [4]. The coastdown methodology captures gearbox, differential, and bearing losses, however, does not account for the speed dependency of the gearbox and bearing losses (i.e. these losses are assumed equal for both speed ranges). On the other hand, the estimation of the speed-dependency of these losses is not necessary for the constant speed test, since it measures the torque directly at the wheels and thus, downstream any frictional losses caused by the powertrain. In summary, both this study and the work done by Rexeis et al. [4] show a difference of 9 and 13%, respectively, between the constant speed and coastdown methods.

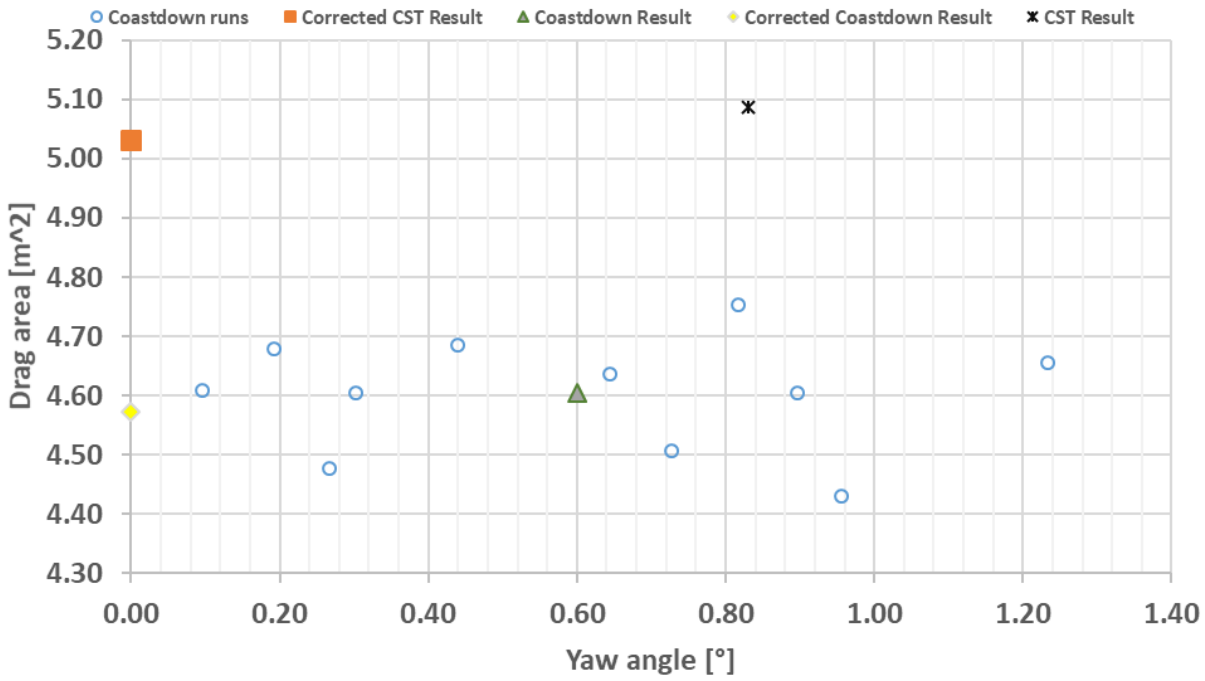

Figure 2.3: Drag area vs. yaw angle for different measurement methods.

2.3 Chassis dynamometer testing

2.3.1 Test Fuel Specifications

WVU used commercially available ultra-low sulfur diesel (ULSD, No. 2 Diesel) fuel originating from the same batch, with specifications meeting those outlined in 40 CFR §1065.70 for testing of the U.S. based vehicle. A list of properties for ULSD fuel used for this study is shown in Table 2.13.

Table 2.13: ULSD test fuel specifications.

ASTM Method	Description	Specifications
D4052	Density @ 15 °C, kg/m^3	830
D4737	Cetane index	51
D-86	Distillation -90% recovered C	282-338
D-445	Viscosity, cSt @ 40 °C	2.0-4.0
D-5453	Sulfur, ppm, max	15
E-482	Ash, mass %, max	0.01
-	Lower heating value (LHV), MJ/kg	42.79

2.3.2 Test Cycles

Five test cycles, namely, the VECTO Long Haul, VECTO Regional Delivery, GEM ARB Transient, GEM 55mph with road grade simulation, and the GEM 55mph without road grade were utilized for chassis dynamometer testing. Figure 2.4 shows the characteristics of speed and road grade profiles required as input for the chassis dynamometer controller.

The VECTO cycles are developed by the European Commission and the details of these cycles are mentioned in the EU regulation 2017/2400 [2]. The VECTO Regional Delivery cycle used in this study is a shortened version of the original one which has a test duration time of 1 hour and 40 minutes. In order to allow for a comparison of the results obtained from this study and the work performed by Rexeis et al. [4], the original VECTO Regional Delivery cycle had to be shortened due to limitations of continuous measurement time on the chassis dynamometer (i.e. chassis dynamometer used by Rexeis et al. [4] was not able to accommodate longer test cycles). Therefore, the same shortened version of the VECTO Regional Delivery was used by WVU. Even though the cycle was shortened, fuel consumption characteristics were conserved compared with its original

cycle. Additional details on the shortening of the VECTO Regional Delivery cycle can be found in the final project report by Rexeis et al. [4].

The GEM ARB Transient cycle does not include road grade simulation and is used for the Phase 1 and Phase 2 GHG standards for HDVs in the US. The constant speed cycle, GEM 55mph, was operated with and without road grade. The GEM 55mph cycle without grade is used in the Phase 1 certification procedure, whereas the GEM 55mph cycle with grade is used in the subsequent Phase 2 certification procedure.

Table 2.14 represents the settings for masses and road load parameters of each test cycle exercised over chassis dynamometer testing. Total test weight of each cycle includes corrections to the reference conditions such as rotational masses of wheels installed on the vehicle. The rolling resistance of the drive tires was evaluated according to the SAE J2452 and the ISO28580 standards to be 4.87N/kN (i.e. using 1.707 meter drum). In order to allow for a comparison to the work performed by Rexeis et al. [4], based solely on aero drag and powertrain influences, the same rolling resistance as Rexeis et al. was selected for the chassis dynamometer testing. The *CdxA* parameter applied for chassis dynamometer testing was 5.031 (i.e. $C_d = 0.481$) obtained from CST.

Table 2.14: Chassis dynamometer test cycle characteristics.

Test Cycle	Payload [1)] (tonnes [2)])	Total testing mass (tonnes)	Rolling resistance used (N/kN)	Distance (km)	Duration (sec)	Average speed (km/h)	Grade (%)	
							min	max
VECTO LH	19.3	36.5	5.5	99.8	4578	90	6.87	6.61
VECTO RD (shortened)	12.9	30.1	5.5	63.2	3587	63.4	6.85	5.66
GEM 55mph w/grade	17.2	34.4	5.5	20	925	86.5	5.01	5.01
GEM 55mph w/o grade	17.2	34.4	5.5	20	925	86.5	N/A	
GEM ARB transient	17.2	34.4	5.5	4.4	690	23.4	N/A	

[1)] *Payloads are defined by the corresponding regulatory tools, i.e. GEM for US and VECTO for EU.*
[2)] *'tonnes' or 'metric ton' is defined as 1000kg.*

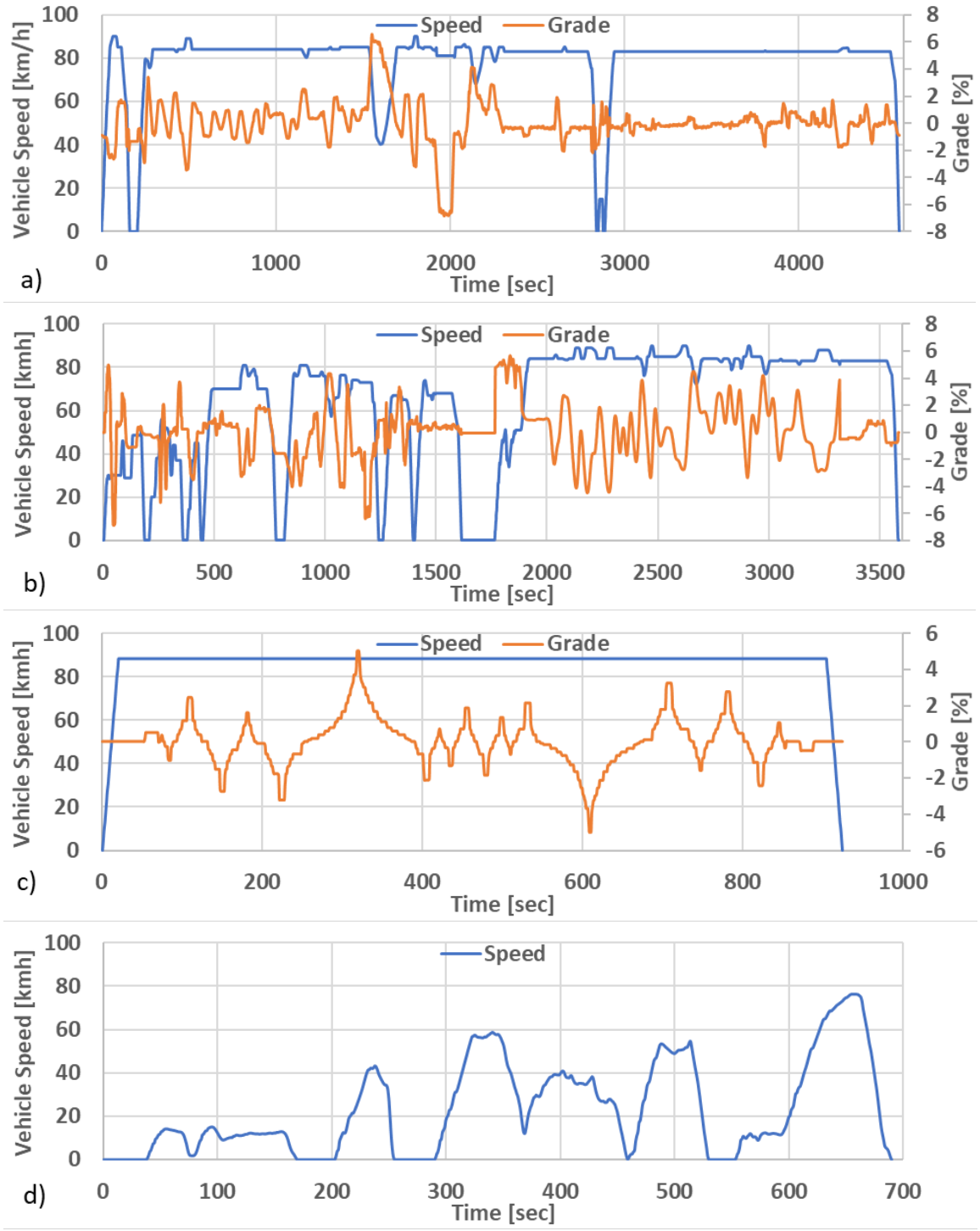

Figure 2.4: Chassis dynamometer test cycles: a) VECTO long haul, b) VECTO regional delivery, c) GEM 55 with grade, and d) GEM ARB transient cycle.

2.3.3 Chassis Dynamometer Measurements

All chassis dynamometer testing for this study was performed this study using California Air Resources Board's (CARB) heavy-duty chassis dynamometer and raw emissions measurement system stationed at CARB's Depot Park facility in Sacramento, CA. This section details the chassis dynamometer and emissions test procedures utilized for the chassis dynamometer testing portion of this study.

2.3.3.1 Chassis Dynamometer Specifications

Table 2.15 provides details of the heavy-duty chassis dynamometer used in this study and located at California ARB's facility (i.e. Depot Park) in Sacramento, CA, USA.

Table 2.15: Specifications of heavy-duty chassis dynamometer at ARB facility, Sacramento, CA.

Make	Burke E. Porter Machinery Company
Test bed type	Twin roller for a single driven axle vehicle
Maximum speed	160 km/h
AC motor configuration	Inline, direct coupled
Max power capacity	480 kW
Vehicle test mass	4.5 to 37 t
Maximum shear brake system	220 kW
Continuous tractive effort	22.7 kN

The measurement systems and parameters used for this study are listed in Table 2.16. Fuel consumption is measured via a gravimetric fuel meter (Ohaus, model 3000). Continuous exhaust emissions concentrations (CO_2, CO, NO, NO_x and THC) were measured with a raw emissions measurement system (AVL i-60 emissions bench), analyzing sample gas by means of NDIR for CO_2 and CO, FID for THC, and CLD in conjunction with a NO_2-to-NO converter for NO and NO_x concentrations, respectively. In addition, a Fourier transform infrared spectrometer (MKS-FTIR, model 2030HS) was used to measure NH_3, CH_4 and other components of interest. A Semtech flow meter was used for raw exhaust flow measurements. The MKS-FTIR 2030HS has a single sample cell with a total absorption length of 5.11m, maintained at 191°C, and can measure raw exhaust emissions in wet conditions. All sampling system components such as sampling lines and heated filters were heated and maintained at 191°C to prevent condensation in the sampling system. The

principle of operation of the MultiGas is based on IR spectroscopy. For a more detailed description of the chassis dynamometer and emissions measurement systems used during this study see [5].

Table 2.16: Measurement systems and parameters [5].

Measurement Parameter	System / Instrument
Vehicle speed, grade, dynamometer force, tractive force, roll acceleration	Burke E. Porter Machinery Company, Chassis dynamometer
Exhaust flow	Semtech HS flow meter
Gravimetric fuel consumption	Ohaus 3000
Engine speed, fuel consumption, engine torque, after-treatment temperature, EGR, current gear, throttle position, vehicle speed	CAN-ECU
THC, NO_x, CO_2, CO	Exhaust gas analyzer AVL- i60, continuous measurement, raw sampling
THC, CO_2, CO, NH_3, CH_4, NO_2, NO	MKS-FTIR 2030, continuous measurement, raw sampling

2.3.4 Test Procedures

The test vehicle was installed and tied down on the chassis dynamometer. Subsequently, the exhaust stack of the vehicle (i.e. lower road side discharge between frame) was connected to the exhaust flow meter via a flexible, 5" transfer pipe. A slip stream was extracted from the sample plane near the exhaust flow meter and routed to the analytical gas measurement systems. Additional weights (i.e. approx. 2 tonnes) were added to the drive axles (i.e. concrete blocks mounted on fifth wheel support) to reduce the probability of tire-roller slippage. Before starting of the chassis dynamometer testing, a dynamometer warm-up procedure was conducted comprising four sets of acceleration and deceleration cycles as shown in Table 2.17. This procedure was performed using the Burke Porter dynamometer warm-up controller with the vehicle placed in neutral gear while the engine was idling.

Table 2.17: Chassis dynamometer warm-up procedure.

Speed Bin	Number of Cycles
Set 1- (64-80 km/h)	25 cycles
Set 2- (32-56 km/h)	25 cycles
Set 3- (88-112 km/h)	25 cycles
Set 4- (16-112 km/h)	25 cycles

Following warm-up of the tire-roller interface and internal roll set bearings, the chassis dynamometer losses were determined by conducting an on-lab coast-down of the vehicle as described in SAE J2264. The target coefficients representative of the truck and trailer combination required for simulation are input into the dynamometer controller software and the automatic coast-down procedure is initiated. The dynamometer software conducts a series of repeated iterative dynamometer controller adjustment to achieve the same coast-down curve as measured over the road. The condition of pass was set for less than 2% error between the target and actual forces measured within 5-mph bins between 60 and 5 mph. The on-dynamometer coast-down determines the dynamometer loss coefficients to determine the magnitude of dynamometer loading that is to be employed to match the target coefficient. Figure 2.5 displays the losses from six repetitions of the chassis dynamometer calibration procedure performed and maximum determined losses differ by some 60 N from all the coastdown runs. This 60 N uncertainty is incorporated into the applied road load forces during measurement of driving cycles. Even though the warm-up procedure was executed properly before the chassis dynamometer coastdown procedure, it was observed that during the first (*orange*) and second (*gray*) coastdown runs as shown in Figure 2.5, losses were higher compared to the runs 3 (*yellow*), 4 (*blue*), and 5 (*green*). This could be explained since further warm-up time was needed for the tire-roller and internal roll-set bearings and could also be related to temperature effects from tires and vehicle drive-line which cannot be fully controlled by a pre-defined warm-up procedure.

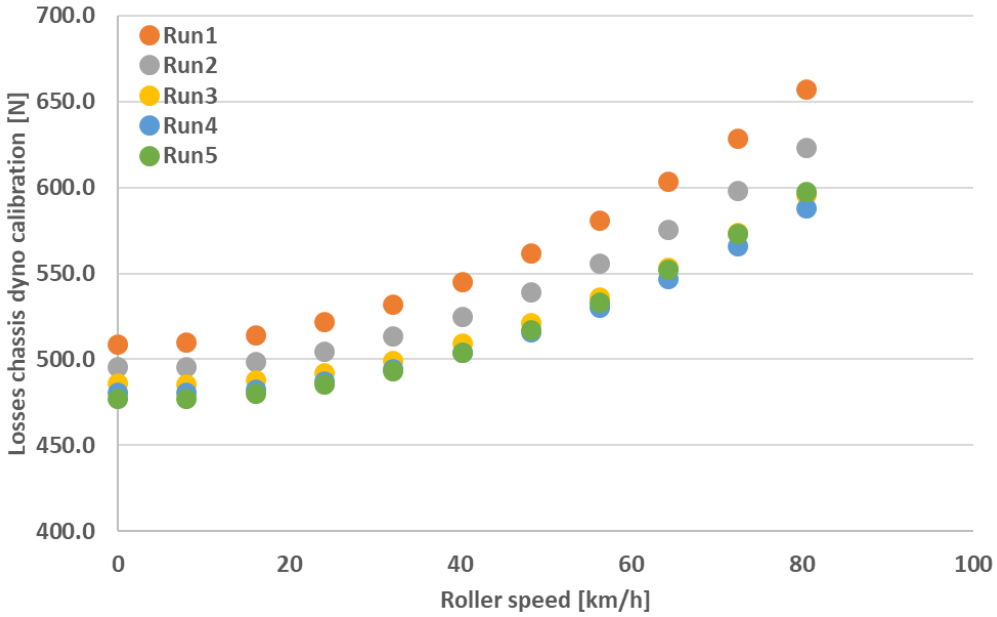

Figure 2.5: Losses estimated from chassis dynamometer calibration procedure.

2.3.4.1 Procedure of chassis dynamometer testing

The chassis dynamometers HDD vehicle testing is performed as follows:

i) Preconditioning:
Each drive cycle was preconditioned by idling vehicle for 10 minutes

ii) External Cooling Fan:
A variable speed (8 to 80 km/h) external cooling fan was applied to vehicle to prevent overheating of the vehicle engine.

iii) Test cell temperature:
Test cell temperature was not controlled during testing and outside temperature was between 23-27 °C during chassis dynamometer testing.

iv) Number of test repeats:
The measurements for each cycle were repeated three times.

2.4 Data evaluation

Emission rates as well as fuel consumption calculations from the different proposed methods including, i) gravimetric measured fuel consumption, ii) ECU broadcasted fuel consumption, iii) calculate via carbon balance from raw exhaust concentration measurements was conducted during the data post-processing stage. Fuel consumption calculations via the different methods mentioned

was performed for data quality purposes. Calculation of emissions mass rates in [g/s] will follow recommendations outlined in regulation 40 CFR 1065.650 and include correction for i) transport delay time in sample lines (i.e. T50 delay time), ii) drift correction for analyzer drift, iii) correction for removed water content for dry exhaust gas measurements (i.e. NO, NO_x, CO_2, and CO). Engine torque and power were calculated based on broadcasted engine control unit (ECU) parameters.

The engine brake torque is not directly broadcasted through ECU and it is determined based on the parameters broadcasted through the J1939 protocol such as actual engine percent torque (AEPT), nominal friction torque (NFPT) and engine reference torque. The engine brake torque can be calculated as shown in Equation 2:

$$T_{brake} = \left[(AEPT - NFPT) * T_{engine\ reference\ torque}\right]/100 \qquad \textbf{Eq. 2}$$

Once the engine brake torque is determined, the engine power and work can be calculated as shown in Equations 3 and 4, respectively, where Δt is the sampling time in (s), T_{brake}, the engine brake torque (Nm), P_{brake} the brake engine power (kW), and W_{brake} the engine brake work (kWh).

$$P_{brake} = brake_{torque} * Speed/9.5488 \qquad \textbf{Eq. 3}$$

$$W_{brake} = [Engine_{Power} * \Delta t]/3600 \qquad \textbf{Eq. 4}$$

The road-load equation used for the total force applied to the vehicle as shown in Equation 5 where M_{test} is the test mass, a is the acceleration and g is the gravimetric constant. The *A* term represents the resistive force that is constant and does not vary with vehicle speed such as tires. The *B* term represents the resistive force that varies linearly with vehicle speed such as drivetrain and differential and the *C* term represents the resistive force that varies with the square of vehicle speed such as wind.

$$\begin{aligned} F = {} & [A + (B * V) + (C * V^2)] \\ & + [(1 + drive\ axle\ \% + non_{drive} axle\ \%) * M_{test} * a] \\ & + [M_{test} * g * \sin(\arctan(grade\%))] \end{aligned} \qquad \textbf{Eq. 5}$$

3 RESULTS AND DISCUSSION

3.1 Average Wheel Work

Figure 3.1 demonstrates the distance-specific positive wheel work results in [kWh/km] over all the test cycles performed during chassis dynamometer testing. Distance-specific Positive wheel work is the ratio between the positive work performed at the wheel, divided by the total distance traveled. In this study, direct wheel hub torque measurements were not available during chassis dynamometer testing, thus only results from VECTO simulations for wheel work are shown in Figure 3.1.

The highest positive distance-specific wheel work was obtained over the ARB Transient cycle, which can be explained due to the higher simulated vehicle test mass (i.e. 17.2 tonnes payload) combined with the highly transient operating characteristics of the cycle. From VECTO simulations, positive distance-specific wheel work was found to be 1.22 and 1.02 for the VECTO Long Haul and the flat (i.e. without grade) GEM 55mph cycles, respectively (see Figure 3.1). In these cycles work demand was lower compared to the work demand observed during the transient GEM cycle (i.e. ARB Transient cycle). Moreover, the flat GEM 55mph cycle does not include any road grade simulation, and thus, as expected, lower positive distance-specific wheel work was observed compared to the GEM 55mph with a road grade profile (i.e. 1.02 vs. 1.15kWh/km).

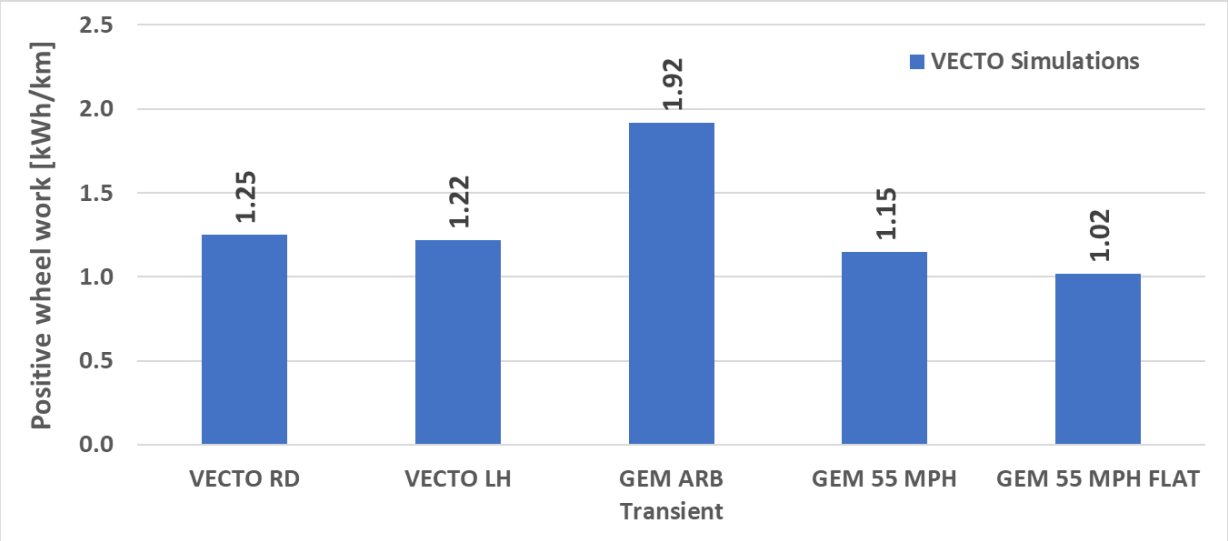

Figure 3.1: Comparison of distance-specific positive wheel work in [kWh/km] between experimental results and simulations for the different chassis dynamometer cycles.

3.2 Fuel Consumption

Figure 3.2 depicts a comparison of the distance-specific fuel consumption in [L/100km] between the gravimetric measured fuel consumption and amount of fuel consumed, calculated based on ECU broadcasted parameters. The gravimetric-based fuel consumption values vary between 24.5 and 64.4 L/100km depending on test cycle.

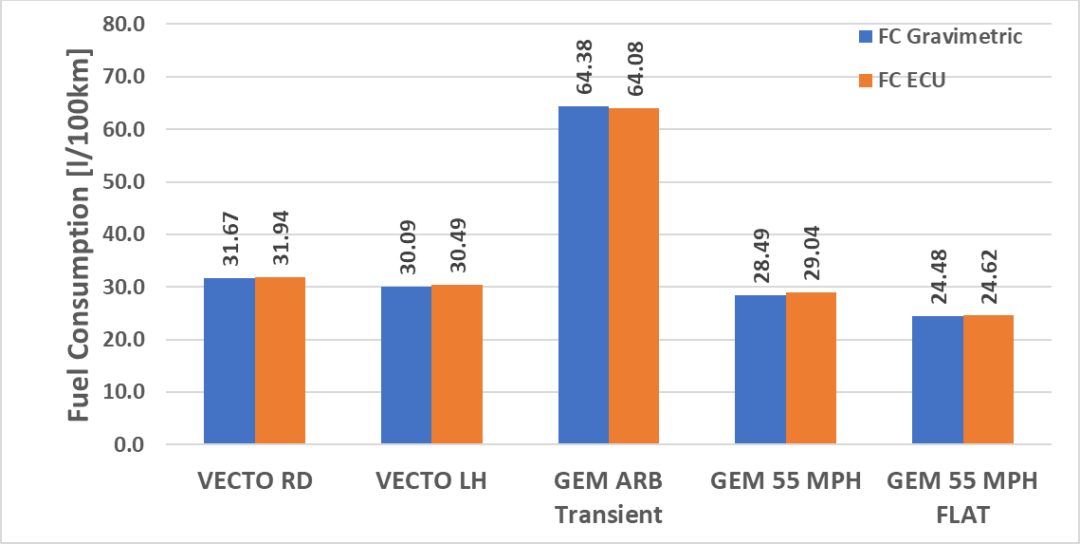

Figure 3.2: Comparison of distance-specific fuel consumption between gravimetric and ECU-broadcasted calculation methods in [L/100km] for the different chassis dynamometer cycles.

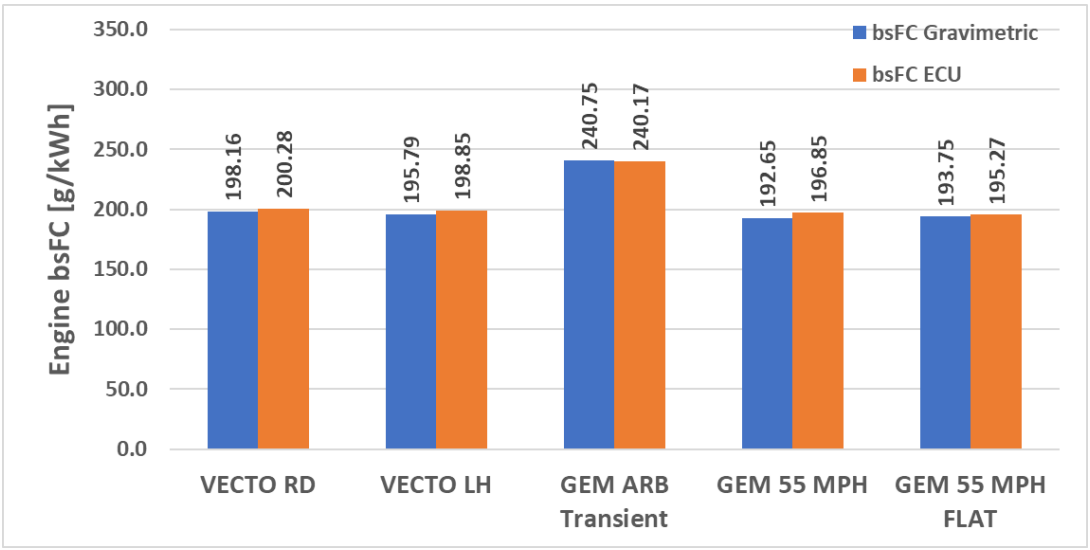

Figure 3.3: Comparison of work-specific fuel consumption between gravimetric and ECU-broadcasted calculation methods in [g/kWh] for the different chassis dynamometer cycles.

Figure 3.4 depicts a comparison of CO_2 mass emissions per ton-kilometer for the different cycles. Highest per ton-kilometer CO_2 emissions were found to be 98.81g/t-km over the ARB

Transient cycle. It is important to demonstrate fuel consumption in terms of CO_2 mass emissions (g/t-km) since this unit is used as a primary metric for certification and limitation of CO_2 emissions from heavy-duty vehicles.

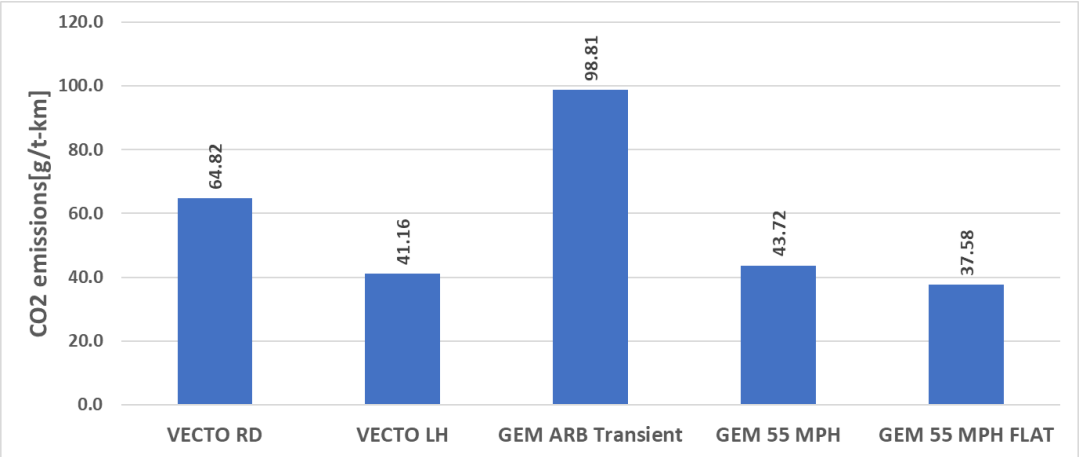

Figure 3.4 Comparison of CO_2 emissions in [g/t-km] between the different chassis dynamometer cycles.

3.3 Steady-state Engine Mapping Results

Steady-state chassis dynamometer testing was performed to evaluate fuel consumption over steady-state engine operating conditions. The test matrix comprised 6 different engine speeds between 800 and 1800rpm with 5 different load points per engine speed equally distributed between 20 and 100% load as seen from Table 3.1.

Table 3.1: Selected steady-state test points.

Engine speed [rpm]	Percent load at given engine speed [%]
1800	100, 80, 60, 40, 20
1600	100, 80, 60, 40, 20
1400	100, 80, 60, 40, 20
1200	100, 80, 60, 40, 20
1000	100, 80, 60, 40, 20
800	100, 80, 60, 40, 20

Figure 3.5 along with Figure 3.6 show brake-specific fuel consumption (bsfc) values calculated from gravimetric and ECU-based fuel measurements, respectively, over the 30 steady-state engine operating modes. It can be seen that engine fuel efficiency is found to be the lowest at the lowest (20%) engine load operating conditions for all engine speed ranges. For a given engine load, bsfc increases with respect to engine speed except for engine speed ranges from 1000 to 1200rpm. This can be explained by the fact that HDD engines are specifically calibrated to operate most efficiently between these engine speed ranges in terms of fuel consumption for both low and high engine load operating conditions. For a given engine speed, bsfc decreases while engine load is increased, thus HDD engines are more efficient while the engine is under higher, sustained load.

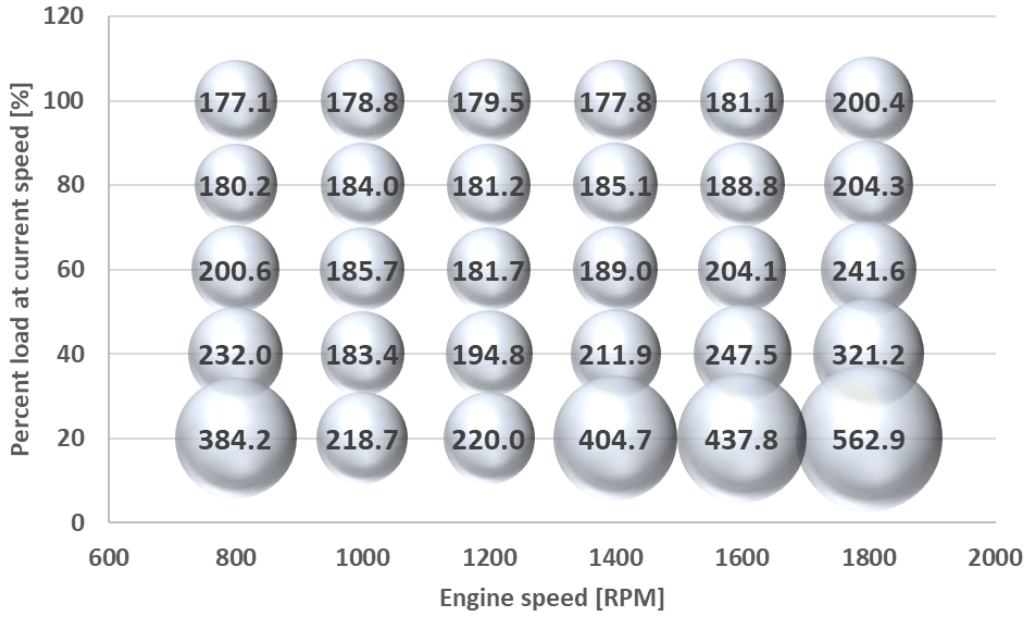

Figure 3.5: Steady-state brake-specific fuel consumption in [g/kWh] calculated through gravimetric fuel measurement and ECU derived engine work.

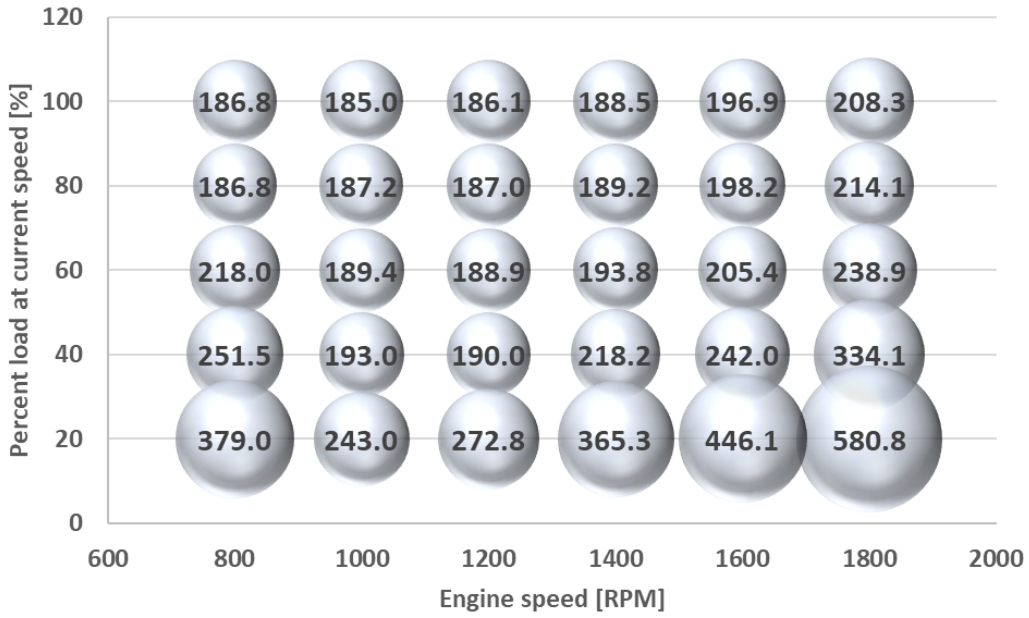

Figure 3.6: Steady-state brake-specific fuel consumption in [g/kWh] calculated through ECU-broadcasted fuel measurement and ECU derived engine work.

Figure 3.7 shows the engine thermal efficiency map obtained from the steady-state chassis dynamometer testing. As expected, it can be observed that engine thermal efficiency increases with an increase in engine load. On average, highest engine thermal efficiency is found to be ~46% at under the engine's full-load condition. In terms of the impact of engine speed on thermal efficiency it can be observed that engine speeds between 1000 to 1400rpm show the highest efficiency, while slowly tapering off towards both higher and lower engine speeds with the exception of 80-100% engine load at the lowest speed point (i.e. 800rpm). This is highly due to manufacturer's successful engine calibration strategy at sustained high engine load (80-100%) while engine operates at low engine speed. Similarly, to the conclusion obtained from the engine fuel map information, the thermal efficiency map supports that engine operate highly efficient during engine speed ranges from 1000 to 1200 rpm.

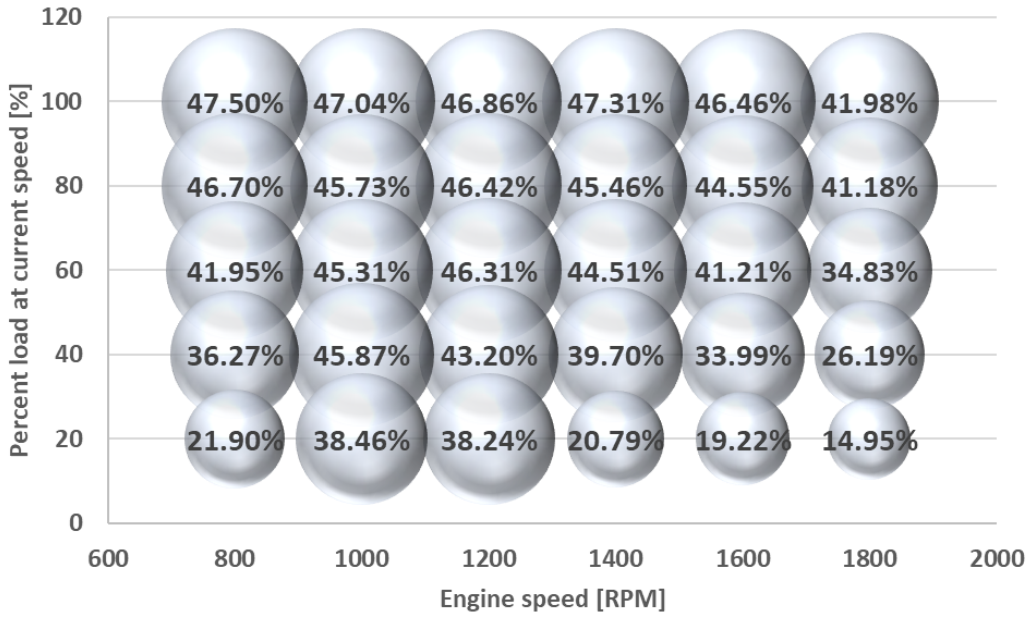

Figure 3.7: Steady-state engine thermal brake efficiency [%] calculated through gravimetric fuel measurement and ECU derived engine work.

4 REFERENCES

1 "Control of Emissions from New Heavy-Duty Motor Vehicles," US Environmental Protection Agency, Federal Register, Title 40, Vol. 1037, Subpart F, §1037.528, accessed: April, 2018.

2 European Commission. (2017). REGULATION (EU) 2017/2400 of 12 December 2017 implementing Regulation (EC) No 595/2009 of the European Parliament and of the Council as regards the determination of the CO2 emissions and fuel consumption of heavy-duty vehicles and amending Directive 2007/46/EC of the European Parliament and of the Council and Commission Regulation (EU) No 582/2011. Official Journal of the European Union, L 349. Retrieved from http://eur-lex.europa.eu/legal-content/EN/TXT/?uri=OJ:L:2017:349:TOC.

3 "Control of Emissions from New Heavy-Duty Motor Vehicles," US Environmental Protection Agency, Federal Register, Title 40, Vol. 1037, Subpart F, §1037.501, accessed: April, 2018.

4 Rexeis, M., Röck, M., and Hausberger, S. (2018). Comparison of fuel consumption and emissions for representative heavy-duty vehicles in Europe (No. FVT-099/17/Rex EM 16/18-6790). Technische Universität Graz. Retrieved from https://www.theicct.org/publications/HDV-EU-fuel-consumption-and-emissions-comparison.

5 Arvind Thiruvengadam et al., "Cross Correlation of ARB Heavy-Duty Chassis Dynamometer Emissions Laboratory with WVU Transportable Emissions Measurement System (TEMS)," Final Project Report, Contract Number 12-536, August, 19th, (2016).